

Study of phase transition in (Pb,Ba)TiO₃ thin films

F. M. Pontes, L. S. Santos, D. S. L. Pontes, E. Longo, S. Claro Neto et al.

Citation: *J. Appl. Phys.* **104**, 014107 (2008); doi: 10.1063/1.2956399

View online: <http://dx.doi.org/10.1063/1.2956399>

View Table of Contents: <http://jap.aip.org/resource/1/JAPIAU/v104/i1>

Published by the [AIP Publishing LLC](#).

Additional information on *J. Appl. Phys.*

Journal Homepage: <http://jap.aip.org/>

Journal Information: http://jap.aip.org/about/about_the_journal

Top downloads: http://jap.aip.org/features/most_downloaded

Information for Authors: <http://jap.aip.org/authors>

ADVERTISEMENT



AIPAdvances

Now Indexed in
Thomson Reuters
Databases

Explore AIP's open access journal:

- Rapid publication
- Article-level metrics
- Post-publication rating and commenting

Study of phase transition in (Pb,Ba)TiO₃ thin films

F. M. Pontes,^{1,a)} L. S. Santos,¹ D. S. L. Pontes,² E. Longo,² S. Claro Neto,³ E. R. Leite,⁴ A. J. Chiquito,⁵ and P. S. Pizani⁵

¹Department of Chemistry, Universidade Estadual Paulista (UNESP), Caixa Postal 473, 17033-360 Bauru, São Paulo, Brazil

²Institute of Chemistry, Universidade Estadual Paulista (UNESP), Caixa Postal 355, 14801-970 Araraquara, São Paulo, Brazil

³Institute of Chemistry of São Carlos, University of São Paulo, P.O. Box 780, 13560-970 São Carlos, São Paulo, Brazil

⁴LIEC-CMDMC-Dept. of Chemistry, Federal University of São Carlos (UFSCar), Rod. Washington Luiz, km 235, CP 676, 13565-905 São Carlos, São Paulo, Brazil

⁵Department of Physics, Federal University of São Carlos (UFSCar), Rod. Washington Luiz, km 235, 13565-905 São Carlos, São Paulo, Brazil

(Received 21 September 2007; accepted 10 May 2008; published online 15 July 2008)

Dielectric and Raman scattering experiments were performed on polycrystalline Pb_{1-x}Ba_xTiO₃ thin films ($x=0.40$ and 0.60) as a function of temperature. The dielectric study on single phase compositions revealed that a diffuse-type phase transition occurred upon transformation of the cubic paraelectric to the tetragonal ferroelectric phase in all thin films, which showed a broadening of the dielectric peak. Diffusivity was found to increase with increasing barium contents in the composition range under study. In addition, the temperature dependence of Raman scattering spectra was investigated through the ferroelectric phase transition. The temperature dependence of the phonon frequencies was used to characterize the phase transitions. Raman modes persisted above the tetragonal to cubic phase transition temperature, although all optical modes should be Raman inactive. The origin of these modes was interpreted as a breakdown of the local cubic symmetry by chemical disorder. The lack of a well-defined transition temperature and the presence of broadbands in some temperature intervals above the paraferroelectric phase transition temperature suggest a diffuse-type phase transition. © 2008 American Institute of Physics. [DOI: 10.1063/1.2956399]

I. INTRODUCTION

In the past few years, ferroelectric thin films, especially those with a perovskite structure, have attracted much interest due to their application in various fields such as nonvolatile memory cells and dynamic random access memories and because of the continuing trend for miniaturization.^{1,2} In all these applications, the fundamental properties and performance of these films are strongly affected by their microstructure, including their grain size, shape, orientation, and distribution. In addition, an important factor for most of these applications is the control of the phase transition temperature. To meet this goal, various (Ba,Sr)TiO₃, Pb(Ti_{1-x}Zr_x)O₃, Ba(Ti_{1-x}Zr_x)O₃, Pb_{1-x}La_xTiO₃, Pb(Sc,Ta)_{1-x}Ti_xO₃, Pb_{1-x}Ca_xTiO₃, and (Pb_{1-x}La_x) × (Ti_{1-x}Zr_x)O₃ thin films have been investigated.³⁻⁷ These materials are either classical or relaxor ferroelectrics, depending on the value of x as well as the occupation of A and B sites in the perovskite structure. One of the characteristics of a relaxor ferroelectric material is the existence of so-called polar nanoregions, which appear far above the T_{\max} temperature of the peak in the dielectric constant.

PbTiO₃ is one of the ferroelectric compounds with the highest transition temperatures when one considers materials with the perovskite-type (ABO₃) structure. It is well known that homovalent and heterovalent substitutions on the A and

B sites give rise to different behaviors such as the relaxor properties. In this case, the prototype PbMg_{1/3}Nb_{2/3}O₃ shows a random cation distribution (Mg²⁺ and Nb⁵⁺) on the B site of the perovskite-type structure, which, in turn, gives rise to local quenched electric random fields. These fields are strong enough to prevent phase transition toward a true long range polar ferroelectric phase.⁸

The Curie temperature of many ferroelectric compounds with perovskite-type structures is nonlinearly dependent on the concentration. Some possible reasons for the nonlinearity may be the limited solubility of components, ion ordering, and influence of the morphotropic phase boundary.⁹ Wang *et al.*¹⁰ reported that Ba_{0.7}Sr_{0.3}TiO₃ thin films grown on LaAlO₃ (001) substrate exhibited an obvious room temperature ferroelectric state, while the film grown on SrTiO₃ (001) showed a broad phase transition peak near room temperature. However, the transition is only broadened without any frequency dispersion.

Zhong and Shiosaki¹¹ reported a study on Bi_{3.25}La_{0.75}Ti₃O₁₂ thin film phase transition, in which the dielectric constant versus temperature curves showed four peak dielectric anomalies. The authors proposed that the peak at 483 °C indicates a phase transition paraferroelectric. Naik *et al.*¹² reported a study on Pb_{0.4}Sr_{0.6}TiO₃ thin films, where the dielectric permittivity versus temperature data showed a broad peak at room temperature, indicating a rather diffuse phase transition. Studies of Ito *et al.*¹³ on bulk Pb_{1-x}Ba_xTiO₃

^{a)}Electronic mail: fenelon@fc.unesp.br.

solid solution showed a diffuse ferroelectric to paraelectric transition associated with a broad $\epsilon(T)$ anomaly over a wide temperature range.

The substitute PbTiO_3 system (mainly on *A* site) resulting in solid solutions of the $\text{PbTiO}_3\text{-CaTiO}_3$ (PCT), $\text{PbTiO}_3\text{-SrTiO}_3$, and $\text{PbTiO}_3\text{-BaTiO}_3$ types have received considerable attention, both in thin films and bulk form, due to a high piezoelectric effect and good ferroelectric and pyroelectric properties.^{14–17} Additions such as Sr^{2+} , Ba^{2+} , or Ca^{2+} are usually employed to decrease the Curie temperature for particular applications and to maintain a fairly low temperature dependence of the dielectric constant. CaTiO_3 is paraelectric at room temperature and PbTiO_3 is ferroelectric; therefore, the addition of Ca^{2+} to PbTiO_3 decreases the Curie temperature.

In this paper, we report an investigation of the temperature dependence of the dielectric permittivity and Raman spectra of $\text{Pb}_{1-x}\text{Ba}_x\text{TiO}_3$ (PBT) thin films prepared by a soft chemical method on Pt-coated silicon substrate.

II. EXPERIMENTAL CONDITIONS

The $\text{Pb}_{0.6}\text{Ba}_{0.4}\text{TiO}_3$ (PBT60) and $\text{Pb}_{0.4}\text{Ba}_{0.6}\text{TiO}_3$ (PBT40) thin films studied here were produced by soft chemical processing. Details of the preparation method can be found in the literature.¹⁸

The polymeric precursor solution was spin-coated onto substrates [Pt(140 nm)/Ti(10 nm)/ SiO_2 (1000 nm)/Si] using a commercial spinner operating at 7000 rev/min for 30 s (spin-coater KW-4B, Chemat Technology) and a syringe filter to avoid particulate contamination. After spinning, the films were kept in ambient air at 150 °C on a hot plate for 20 min to remove residual solvents. A two-stage heat treatment was carried out: initial heating at 400 °C for 4 h at a heating rate of 5 °C/min to pyrolyze the organic materials, followed by heating at 600 °C for 2 h for crystallization. The film thickness was controlled by adjusting the number of coatings; the coating/drying operation was repeated until the desired thickness was achieved.

Electrical measurements were taken on PBT60 and PBT40 thin films with 480 and 300 nm thicknesses, respectively. The temperature-dependent dielectric constant of the thin film was studied in metal-ferroelectric-metal configuration, and the film was characterized using a Keithley 3330 (LCR) meter in the temperature range of 298–653 K. The capacitance-voltage (*C-V*) curves were measured using an HP4194A impedance/gain phase analyzer in the temperature range of 298–573 K. For these measurements, circular Au electrodes of approximately $4.9 \times 10^{-2} \text{ mm}^2$ area were deposited (using a shadow mask) by evaporation process on the surfaces of the heat-treated films as top electrodes.

The Raman measurements were taken with a T-64000 Jobin-Yvon triple monochromator coupled to a charge-coupled device detector. An optical microscope with a 50× objective was used to focus the 514.5 nm line of Coherent Innova 90 argon laser into the sample. The power was kept at 20 mW. A TMS 93 oven (Linkam Scientific Instruments Ltd.) was used under the microscope for the measurements in the 298–673 K temperature range.

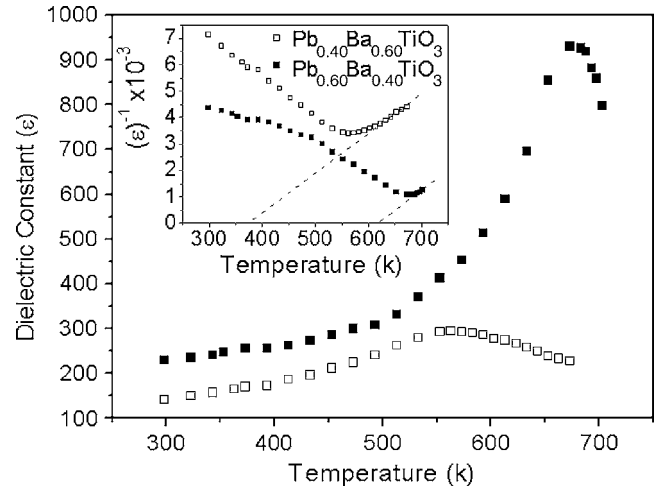


FIG. 1. Variation of dielectric constant with temperature of $\text{Pb}_{1-x}\text{Ba}_x\text{TiO}_3$ thin films at 100 kHz. The inset shows the inverse of the dielectric constant ($1/\epsilon$) as a function of temperature. ■ $\text{Pb}_{0.60}\text{Ba}_{0.40}\text{TiO}_3$; □ $\text{Pb}_{0.40}\text{Ba}_{0.60}\text{TiO}_3$.

III. RESULTS

Several interesting features are apparent from the dielectric constant (ϵ) versus temperature curves of PBT60 and PBT40 thin films with different Ba^{+2} concentrations (see Fig. 1). Irrespective of the Ba^{+2} concentrations, a broad maximum of dielectric constant (ϵ) is observed indicating the diffuse nature of the phase transition with increasing Ba^{+2} concentration. The strongly broadened dielectric peak indicates that the phase transition is of a diffuse type near the transition temperature; this may be caused by (i) inhomogeneous distribution of barium ions on lead site or (ii) mechanical stress in the grain. In addition, Fig. 1 shows that the transition temperatures also shift downward with increasing barium content.

For a normal ferroelectric in the vicinity of the transition temperature, the dielectric stiffness ($1/\epsilon$) follows the well-known Curie–Weiss law¹⁹

$$\epsilon = C/(T - T_0), \quad (1)$$

where C is the Curie–Weiss constant and T_0 is the Curie–Weiss temperature.

In addition, the order of the ferroelectric to paraelectric phase transition can be determined from the temperature dependence of the dielectric constant inverse ($1/\epsilon$). When T_0 is lower than T_C , we observe a first order transition; on the other hand, when $T_0 = T_C$, a second order transition is observed.²⁰

The inset in Fig. 1 shows the temperature behavior of the inverse of the dielectric constant at 100 kHz for the PBT thin films. The parameters C and T_0 were fitted in a narrow temperature range near T_C . Both the ferroelectric to paraelectric phase transition temperature (T_C) and the Curie–Weiss temperature (T_0) can be obtained directly from these data. The best fitting parameters are $C = 1.18 \times 10^5 \text{ K}$ and $T_0 = 602 \text{ K}$ and $C = 1.34 \times 10^5 \text{ K}$ and $T_0 = 343 \text{ K}$ for PBT60 and PBT40 thin films, respectively. The Curie–Weiss temperature for both thin films is lower than the transition temperature, as expected from the first order phase transition between the paraelectric and ferroelectric phases. For PBT60 and PBT40

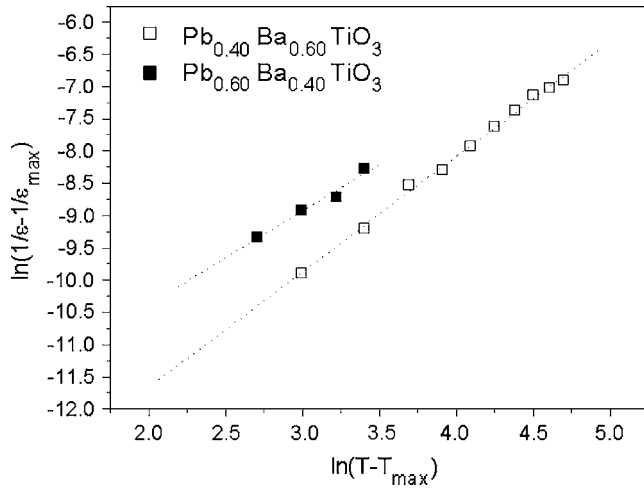


FIG. 2. Plot of $\ln(1/\varepsilon - 1/\varepsilon_{\max})$ as a function of $\ln(T - T_c)$ for $\text{Pb}_{1-x}\text{Ba}_x\text{TiO}_3$ thin films with different compositions.

thin films the transition temperatures were 673 and 563 K, respectively. This result is congruent with the conclusion of Guilloux-Viry *et al.*,²¹ who found that the Curie–Weiss temperature was lower than T_C , suggesting that the transition is of first order, as determined from dielectric measurements taken on $\text{SrBi}_2\text{Nb}_2\text{O}_9$ thin films grown by pulsed laser on Pt electrodes. In addition, the Curie constants obtained here are typical values for a wide variety of displacement-type ferroelectric phase transitions. On the other hand, ordered-disordered-type ferroelectric phase transitions tend to have a Curie constant of about $C \sim 10^3$ K.¹⁹ Recently, Tyunina and Levoska²² reported that $\text{Ba}_{0.50}\text{Sr}_{0.50}\text{TiO}_3$ thin films on Pt- Al_2O_3 substrates showed a relaxorlike nature of the dielectric peak. The Curie–Weiss law behavior observed by the authors reported values of $C = 0.75 \times 10^5$ K and $T_0 = 245$ K for the $\text{Ba}_{0.50}\text{Sr}_{0.50}\text{TiO}_3$ thin films deposited at 1073 K by pulsed laser deposition (PLD).

In $\text{Pb}_{1-x}\text{Ba}_x\text{TiO}_3$ thin films, an enhanced diffuse behavior is expected when the amount of different substitute cations on the A site is increased. Taking into account that the PBT40 thin film showed a broad maximum dielectric constant, a modification in the Curie–Weiss law is necessary. In the literature, an empirical modification of the Curie–Weiss law was proposed to describe the diffuseness of the phase transition as follows:²³

$$1/\varepsilon - 1/\varepsilon_m = (T - T_{\varepsilon_{\max}})^{\gamma}/C^*, \quad (2)$$

where γ is the critical exponent measuring the degree of diffuseness of the transition and C^* is a Curie–Weiss like constant. For a sharp transition, $\gamma = 1$, and for a diffuse transition it lies in the range $1 < \gamma \leq 2$. The plot of $\ln[1/\varepsilon - 1/\varepsilon_{\max}]$ vs $\ln[T - T_c]$ at 100 kHz for two different compositions is shown in Fig. 2. Linear dependencies are observed. The slopes of the fitting curve are used to determine the value of the γ parameter. The values of γ at 100 kHz are found to be 1.44 and 1.78 for PBT60 and PBT40 thin films, respectively, indicating that the transitions are of a diffuse nature. Pokharel and Pandey²⁴ reported values of γ in the range of 1.25–1.50 for the diffuse behavior of the $(\text{Pb}_{1-x}\text{Ba}_x)\text{ZrO}_3$ system. In addition, Ganesh and Goo²⁵ re-

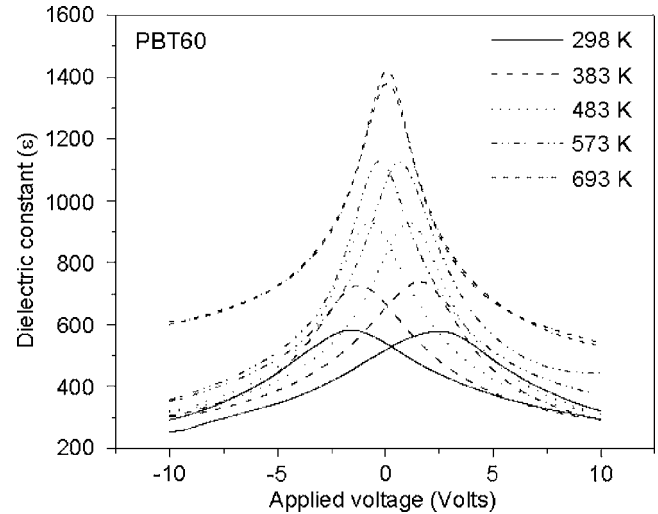


FIG. 3. Curves of the ε -V characteristics of the PBT60 thin film at different temperatures at 100 kHz.

ported values of γ in the range of 1.20–1.34 for the diffuse behavior of the paraelectric-ferroelectric transition region for the $(\text{Pb}_{1-x}\text{Ca}_x)\text{TiO}_3$ system.

The strong diffuseness of the PBT40 thin film can be attributed to the microscopic inhomogeneity and/or smaller grain size that may have stress-induced the region near the film electrode and/or grain boundary interfaces. In addition, the large broadness observed in PBT40 thin film can also occur due to structural disordering in the arrangement of cations in one or more crystallographic sites of the perovskite structure. The diffuse character of the transition increases as the grain size decreases from 140 in PBT60 to 100 nm in PBT40 thin films. Therefore, we believe that the presence of a submicron size grain in $\text{Pb}_{0.4}\text{Ba}_{0.6}\text{TiO}_3$ thin film causes intergranular stress, which leads to a broadened maximum in the temperature dependence of the dielectric constant (γ). This behavior was observed mainly in the PBT40 thin films with a grain size of approximately 100 nm. According to Park *et al.*,²⁶ the particle size influences the ferroelectric transition of the BaTiO_3 . The value of T_c decreases gradually, but the transition becomes diffuse as the particle size decreases from 81 to 40 nm. Jimenez and Jimenez²⁷ recently predicted a diffusive nature for the ferroelectric phase transition of $x = 0.45$ for PCT ceramic using dielectric data. The dielectric results for $x = 0.45$ were $\gamma = 1.62$. In addition, Zhai *et al.*²⁸ reported a diffusive phase transition accompanied by relaxor behavior for $\text{Ba}(\text{Zr}_x\text{Ti}_{1-x})\text{O}_3$ thin films grown by a sol-gel process. Similar relaxor behavior to epitaxial heterostructures of $\text{Ba}_{0.80}\text{Sr}_{0.20}\text{TiO}_3$ thin film growth by PLD on MgO (001) single-crystal substrates using $\text{La}_{0.5}\text{Sr}_{0.5}\text{CoO}_3$ as a bottom electrode was reported by Tyunina and Levoska.²⁹ In addition, the authors observed a coexistence of both ferroelectriclike and relaxorlike behavior analyses based on the difference in the dynamic nonlinear dielectric responses of normal ferroelectrics and relaxors.

Figures 3 and 4 show the dielectric constant-voltage (ε -V) curves of $\text{Pb}_{1-x}\text{Ba}_x\text{TiO}_3$ thin films deposited on Pt/Ti/SiO₂/Si substrate. The ε -V curves were obtained at different temperatures at 100 kHz, with oscillation amplitude

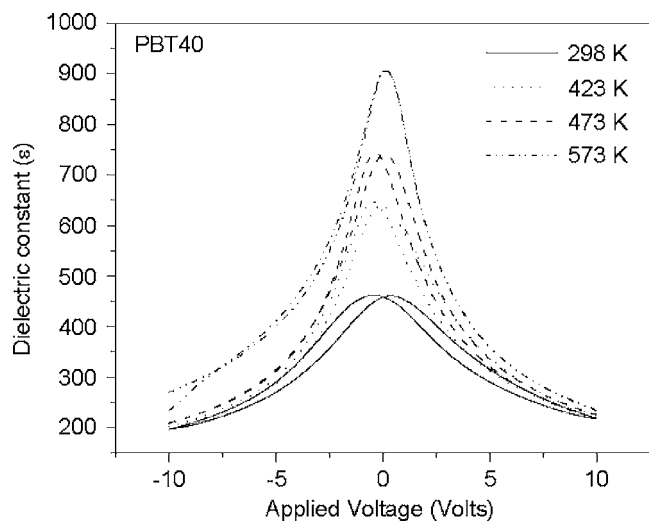


FIG. 4. Curves of the ϵ - V characteristics of the PBT40 thin film at different temperatures at 100 kHz.

of 50 mV. The capacitance of the films showed a strong dependence on the applied voltage. The ϵ - V curve showed two broad peaks at 298 K and was symmetric about the zero-bias axis. All the thin films displayed a hysteresis behavior. Increasing the temperature caused the butterfly shape of the curves to decrease. The gap between the ϵ - V curves of the positive and negative biases was reduced; the curves showed absence of splitting (butterfly type) at decreasing/increasing voltages for both polarities at about 693 and 573 K for PBT60 and PBT40 thin films, respectively. This fact indicates that the temperatures of 693 and 573 K correspond to the ferroelectric-paraelectric phase transition temperatures.

To study the ferroelectric to paraelectric phase transition by Raman spectroscopy, Raman spectra of $\text{Pb}_{1-x}\text{Ba}_x\text{TiO}_3$ thin films were obtained at different temperatures, and the results are shown in Figs. 5 and 6. The room temperature Raman spectra of all thin films were found to be congruent with the literature, showing all expected Raman-active optical modes. Increasing the temperature caused a decrease in

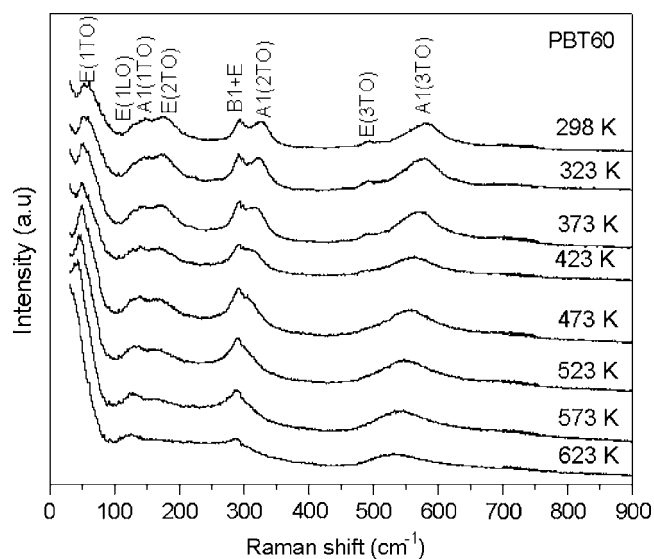


FIG. 5. Raman spectra of PBT60 thin film as a function of temperature.

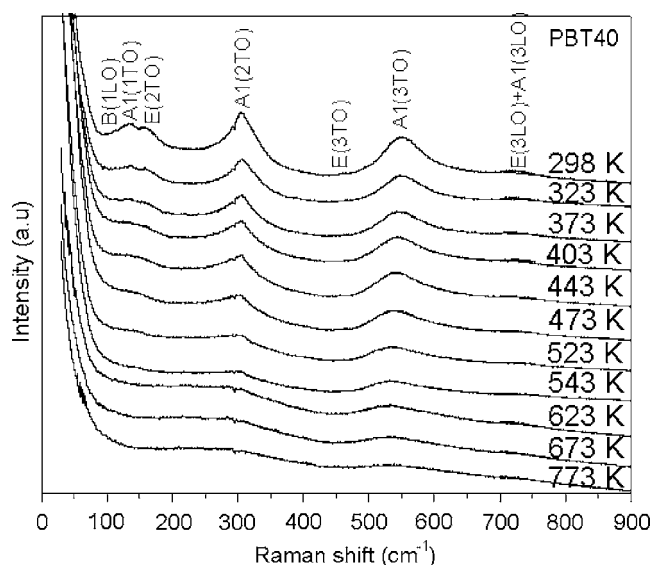


FIG. 6. Raman spectra of PBT40 thin film as a function of temperature.

the intensity and a broadening of the Raman peaks. However, some important features in Raman peaks disappear completely at a certain critical temperature corresponding to the ferroelectric to paraelectric phase transition temperature. Conversely, some peaks persist even at temperatures above the transition. Figure 7 shows the temperature dependence of the $E(1\text{TO})$ lowest-frequency Raman mode for PBT60 thin films, whose frequency goes to zero at about 623 K, as indicated in Fig. 5. This typical soft mode behavior is responsible for the ferroelectric to paraelectric phase transition. Furthermore, important information can be obtained from a detailed examination of the temperature dependence of the soft mode line shape in the light of the damped classical harmonic oscillator model. In order to properly determine the damping factor γ as a function of temperature, the Raman intensity was described according to the following equation:³⁰

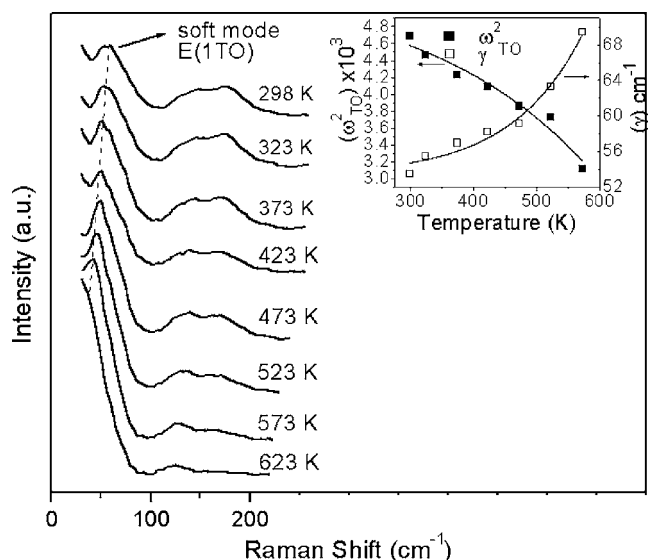


FIG. 7. Low-frequency Raman spectra of $\text{Pb}_{0.60}\text{Ba}_{0.40}\text{TiO}_3$ thin film as a function of temperature. The inset shows the temperature dependence of the $E(1\text{TO})$ mode peak frequency (ω_{TO}^2) and damping factor γ as deduced from Eq. (3).

$$I(\omega) \propto \frac{KTP_s \varepsilon'(0) \gamma \omega_{\text{TO}}^2}{(\omega_{\text{TO}}^2 - \omega^2)^2 + \gamma^2 \omega^2}, \quad (3)$$

where P_s is the spontaneous polarization and $\varepsilon'(\omega)$ is the real part of the dielectric constant.

Equation (3) was fitted to the experimental data, and the damping factors γ were obtained for the soft mode $E(1\text{TO})$ for PBT60 thin film as a function of temperature, as displayed in the inset of Fig. 7. With regard to the damping factor, a remarkable increase was observed near the phase transition temperature. Such an increase in damping is observed in a wide range of solid solution perovskite ferroelectrics for the soft mode $E(1\text{TO})$. A similar finding was reported by Yu *et al.*³¹ in $\text{SrBi}_2\text{Ta}_2\text{O}_9$ nanoparticles and by Dobal *et al.*³² in lead titanate thin films on sapphire.

A different value for the transition phase temperature was estimated from the temperature dependence of the damping factor using the damped classical oscillator model. The transition temperature thus determined was about 573 K, i.e., lower than that determined by electrical measurements. Above this temperature, as can be seen in Figs. 5 and 7, the temperature dependence of the damping factor of the $E(1\text{TO})$ mode was not well fitted; therefore, it was impossible to fit the data over 573 K. Fu *et al.*³³ reported similar phonon mode behaviors for PbTiO_3 thin films deposited on Pt/Si substrates, whose transition phase temperature was estimated by the damping factor. Pontes *et al.*³⁴ reported similar behaviors in $\text{Pb}_{0.7}\text{Sr}_{0.3}\text{TiO}_3$ thin films.

In addition, the temperature dependence of the square of the soft mode frequency is also shown in the inset of Fig. 7. However, we can see that, in the case of PBT60 thin film, the persistence of phonon modes well beyond the transition temperature is due to a short-range structural disorder in the paraelectric cubic phase. This disorder destroys the perfect local cubic symmetry, thus allowing Raman activity in the paraelectric phase. The disappearance of the 57 cm^{-1} soft modes at about 573–623 K indicates that the transformation from the ferroelectric to the paraelectric phase occurs in this temperature range, which is consistent with the Curie temperature determined by the electrical characterization (Fig. 1).

On the other hand, the structural modification of PBT40 thin film doped with 60% barium content investigated by Raman scattering measurements shows some facts that can be ascertained from the temperature-dependent Raman spectra: (i) the tetragonal to cubic transition temperature remains difficult to identify from the measured spectra and (ii) was not possible to follow the evolution of the soft mode.

IV. CONCLUSIONS

We studied the temperature dependence of the dielectric constant and Raman spectra of polycrystalline $\text{Pb}_{1-x}\text{Ba}_x\text{TiO}_3$ ($x=0.40$ and 0.60) thin films over a wide range of temperatures. We showed the diffuse nature of the ferroelectric to paraelectric phase transition, which increased with increasing Ba^{+2} content. This behavior was attributed to the effects of grain size and local structural disorder. The γ parameter showed a strong dependence on the Ba^{+2} content. However,

the dielectric study revealed that both the PBT60 and PBT40 thin films were of the classic ferroelectric type and underwent a diffuse-type ferroelectric phase transition. We also used Raman scattering to probe the characteristics of the phase transition. The transition temperature was estimated using the softening of the lowest $E(1\text{TO})$ transverse optical modes, whose results were in good agreement with those of the electric measurements. We also found that broad Raman bands can be seen to persist above the transition temperature in our thin films. This was attributed to the breakdown of selection rules due to the presence of local structural disorder in the paraelectric phase caused by inhomogeneous distribution in the A site of the ABO_3 -type perovskite structure. Finally, the Raman results and electrical measurements indicated that the phase transition in $\text{Pb}_{1-x}\text{Ba}_x\text{TiO}_3$ thin films was of a diffuse nature.

ACKNOWLEDGMENTS

The authors gratefully acknowledge the financial support of the Brazilian financing agencies FAPESP/CEPID (FAPESP Process No. 06/53926-4).

- ¹R. Waser and A. Rudiger, *Nat. Mater.* **3**, 81 (2004).
- ²D. D. Fong, B. Stephenson, K. S. Streiffer, A. J. Eastman, O. Auciello, H. P. Fuoss, and C. Thompson, *Science* **304**, 1650 (2004).
- ³H. Kim, H. J. Kim, and K. W. Choo, *J. Eur. Ceram. Soc.* **25**, 2253 (2005).
- ⁴H. X. Zhu, J. Li, and N. D. Zheng, *Appl. Phys. Lett.* **90**, 1429131 (2007).
- ⁵X. J. Meng, D. Rémiens, M. Detalle, B. Dkhil, J. L. Sun, and J. H. Chu, *Appl. Phys. Lett.* **90**, 1329041 (2007).
- ⁶Y. Xia, C. Cai, X. Zhi, B. Pan, D. Wu, X. Meng, and Z. Liu, *Appl. Phys. Lett.* **88**, 1829091 (2006).
- ⁷D. Y. Wang, Y. L. Cheng, J. Wang, X. Y. Zhou, H. L. W. Chan, and C. L. Choy, *Appl. Phys. A: Mater. Sci. Process.* **81**, 1606 (2005).
- ⁸W. Westphal, W. Kleemann, and M. J. Glinchuk, *Phys. Rev. Lett.* **68**, 847 (1992).
- ⁹V. A. Isupov, *Phys. Status Solidi A* **181**, 211 (2000).
- ¹⁰D. Y. Wang, J. Wang, H. L. W. Chan, and C. L. Choy, *J. Appl. Phys.* **101**, 0435151 (2007).
- ¹¹N. Zhong and T. Shiosaki, *J. Appl. Phys.* **100**, 0341071 (2006).
- ¹²V. M. Naik, D. Haddad, R. Naik, J. Mantese, N. W. Schubring, A. L. Micheli, and G. W. Auner, *J. Appl. Phys.* **93**, 1731 (2003).
- ¹³Y. Ito, S. Shimada, J. I. Takahashi, and M. Inagaki, *J. Mater. Chem.* **7**, 781 (1997).
- ¹⁴S. C. Pillai, S. W. Boland, and S. M. Haile, *J. Am. Ceram. Soc.* **87**, 1388 (2004).
- ¹⁵H. Xu, M. Shen, L. Fang, D. Yao, and Z. Gan, *Thin Solid Films* **493**, 197 (2005).
- ¹⁶I. Bretos, R. Jimenez, M. L. Calzada, M. K. Van Bael, A. Hardy, D. Van Genechten, and J. Mullens, *Chem. Mater.* **18**, 6448 (2006).
- ¹⁷F. M. Pontes, D. S. L. Pontes, E. R. Leite, E. Longo, A. J. Chiquito, P. S. Pizani, and J. A. Varela, *J. Appl. Phys.* **94**, 7256 (2003).
- ¹⁸F. M. Pontes, S. H. Leal, M. R. M. C. Santos, E. R. Leite, E. Longo, L. E. B. Soledade, A. J. Chiquito, M. A. C. Machado, and J. A. Varela, *Appl. Phys. A: Mater. Sci. Process.* **80**, 875 (2005).
- ¹⁹M. E. Lines and A. M. Glass, *Principles and Applications of Ferroelectrics and Related Materials* (Clarendon Press-Oxford, 24, 1977).
- ²⁰J. F. Scott, *Ferroelectric Memories* (Springer Series in Advanced Microelectronics, 7, 2000).
- ²¹M. Guilloux-Viry, J. R. Duclère, A. Rousseau, A. Perrin, D. Fasquelle, J. C. Carru, E. Cattani, C. Soyer, and D. Rémiens, *J. Appl. Phys.* **97**, 114102 (2005).
- ²²M. Tyunina and J. Levoska, *J. Appl. Phys.* **101**, 084119 (2007).
- ²³S. K. Rout, E. Sinha, S. Panigrahi, J. Bera, and T. P. Sinha, *J. Phys. Chem. Solids* **67**, 2257 (2006).
- ²⁴B. P. Pokharel and D. Pandey, *J. Appl. Phys.* **88**, 5364 (2000).

- ²⁵R. Ganesh and E. Goo, *J. Am. Ceram. Soc.* **89**, 653 (1997).
- ²⁶Y. Park, W. J. Lee, and H. G. Kim, *J. Phys.: Condens. Matter* **9**, 9445 (1997).
- ²⁷B. Jiménez and R. Jiménez, *Phys. Rev. B* **66**, 014104 (2002).
- ²⁸J. W. Zhai, D. Hu, X. Yao, Z. K. Xu, and H. Chen, *J. Eur. Ceram. Soc.* **26**, 1917 (2006).
- ²⁹M. Tyunina and J. Levoska, *Phys. Rev. B* **70**, 132105 (2004).
- ³⁰G. Burns and B. A. Scott, *Phys. Rev. B* **7**, 3088 (1973).
- ³¹T. Yu, Z. X. Shen, W. S. Toh, J. M. Xue, and J. Wang, *J. Appl. Phys.* **94**, 618 (2003).
- ³²P. S. Dobal, S. Bhaskar, S. B. Majumder, and R. S. Katiyar, *J. Appl. Phys.* **86**, 828 (1999).
- ³³D. S. Fu, H. Iwazaki, H. Suzuki, and K. Ishikawa, *J. Phys.: Condens. Matter* **12**, 399 (2000).
- ³⁴F. M. Pontes, S. H. Leal, E. R. Leite, E. Longo, P. S. Pizani, A. J. Chiquito, and J. A. Varela, *J. Appl. Phys.* **96**, 1192 (2004).